Cytometry
PART A
Journal of the International Society for Advancement of Cytometry

Semiautomated Analysis of Embryoscope Images: Using Localized Variance of Image Intensity to Detect Embryo Developmental Stages

Anna Mölder,[1*] Sarah Drury,[2] Nicholas Costen,[1] Geraldine M. Hartshorne,[2] Silvester Czanner[1]

[3]School of Computing, Mathematics and Digital Technology, Faculty of Science and Engineering, Manchester Metropolitan University, Manchester, UK

[2]Division of Reproductive Health, Warwick Medical School, University of Warwick, and Centre for Reproductive Medicine, University Hospitals Coventry and Warwickshire NHS Trust, Coventry, United Kingdom

Received 17 June 2014; Revised 12 November 2014; Accepted 27 November 2014

Grant sponsor: Manchester Metropolitan University

Grant sponsor: The Biomedical Research Unit in Reproductive Health

Grant sponsor: University Hospitals Coventry and Warwickshire NHS Trust

Grant sponsor: Warwick Medical School

Additional Supporting Information may be found in the online version of this article.

*Correspondence to: Anna Mölder; School of Computing, Mathematics and Digital Technology, Manchester Metropolitan University, John Dalton Building, Chester Street, Manchester M1 5GD, UK. E-mail: anna.molder@mmu.ac.uk

Published online 16 January 2015 in Wiley Online Library (wileyonlinelibrary.com)

DOI: 10.1002/cyto.a.22611

Abstract

Embryo selection in in vitro fertilization (IVF) treatment has traditionally been done manually using microscopy at intermittent time points during embryo development. Novel technique has made it possible to monitor embryos using time lapse for long periods of time and together with the reduced cost of data storage, this has opened the door to long-term time-lapse monitoring, and large amounts of image material is now routinely gathered. However, the analysis is still to a large extent performed manually, and images are mostly used as qualitative reference. To make full use of the increased amount of microscopic image material, (semi)automated computer-aided tools are needed. An additional benefit of automation is the establishment of standardization tools for embryo selection and transfer, making decisions more transparent and less subjective. Another is the possibility to gather and analyze data in a high-throughput manner, gathering data from multiple clinics and increasing our knowledge of early human embryo development. In this study, the extraction of data to automatically select and track spatio-temporal events and features from sets of embryo images has been achieved using localized variance based on the distribution of image grey scale levels. A retrospective cohort study was performed using time-lapse imaging data derived from 39 human embryos from seven couples, covering the time from fertilization up to 6.3 days. The profile of localized variance has been used to characterize syngamy, mitotic division and stages of cleavage, compaction, and blastocoel formation. Prior to analysis, focal plane and embryo location were automatically detected, limiting precomputational user interaction to a calibration step and usable for automatic detection of region of interest (ROI) regardless of the method of analysis. The results were validated against the opinion of clinical experts.

Key terms

Key terms: automated image analysis; image-based embryo classification; computer-aided diagnosis; automated annotation; time-lapse microscopy; embryoscope; embryology

IN vitro fertilization (IVF) has been in clinical use for more than 30 years. Nevertheless, there is scope for improvement of the embryo selection procedure. By refining selection based on a greater understanding of embryo quality, we could not only reduce multiple births but also save patients the cost and distress of multiple failed attempts. Time-lapse imaging of embryos offers the prospect of such improvements and recent advances in incubator and imaging technology have enabled frequent observation and image capture of individual embryos at intervals of a few minutes. However, with the increased amount of generated imaging data, it is essential to find quality markers suitable for automated detection via computer-aided diagnostic tools. This technology has also opened up a new area of research studying the impact

ISAC
International Society for Advancement of Cytometry

of timing of key occurrences in embryo development. Currently, key events require to be identified and annotated manually, which is time consuming and limits the usefulness of the instrumentation. Noninvasive markers suitable for computer-aided diagnosis are being sought to standardize embryo selection procedures, speed up the annotation process, and provide diagnostic support.

Embryo quality is well known to relate to embryo morphology (1–3) but is not sufficiently precise an indicator to predict outcome reliably in individual patients. Embryo evaluation today is commonly undertaken using annotations of relevant features by experts at intermittent time points during development. Attempts have been made to standardize manual selection (4) and decision support systems exist for evaluating embryos (5–9). However, manual annotation is time consuming, the evaluation will vary according to the observer, and the different clinical conventions used (10). Automatic procedures to aid annotation would make the analysis less subjective and greatly reduce the manual workload involved.

Many reports have highlighted the need to observe embryo development dynamically (11–15). To thoroughly assess the benefits and drawbacks of time-lapse embryo imaging, large scale randomized clinical studies need to be performed, but before they can be done, at least two vital steps remain: The identification of the most promising markers to use and the setup of a system capable of collecting and analyzing large amounts of embryo data in a standardized and robust manner and consistency in evaluation is crucial to the usefulness of results. When migrating from a manual to an automated system, it may not be possible to require 1:1 correspondence between measurements, if the two selections are made based on distinctly different criteria. In these cases, a comparison must be made between manual and automatic evaluation, to establish the presence and size of any offset. Such comparative studies will need not only expertise in current methodology in both current embryo selection procedures and manual annotation but also a firm understanding of computerized image analysis and the nature of the image material used.

Several systems for automated embryo analysis using various approaches have previously been reported. One time-lapse system available uses an image-based decision tool analyzing cleavages to the four-cell stage using dark field optics (16). A few systems rely on direct modeling of physical conditions (17,18), requiring a highly controlled environment as well as detailed knowledge of the optical setup, something which is not always possible under clinical conditions. Other systems perform pattern recognition on microscopic images. Usually, a correctly performed segmentation (18–21) provides the most detailed information on blastomere position, shape, and outline, but this can be prone to errors, especially when used under clinical circumstances where complete and accurate segmentation may not always be possible. Using a semi-automatic approach, where a region of interest (ROI) has been selected manually (22–24); it is often possible to perform various computer vision and pattern recognition tasks even in a clinical setting. However, with a manual input required to initialize computation, this approach may instead increase user interaction with images, making it more suitable for indepth research purposes than for routine clinical work or large scale studies.

As an alternative, this study investigates the possibility of accessing relevant information using variations in image gray level in bright field images. The result is a framework for the detection of key events in embryo development without requiring samplewise initialization. At the same time, a graphical interpretation of embryo development as viewed in vitro is presented, serving as a complement to manual inspection of images.

Materials and Methods

Embryo Culture and Image Capture

Time-lapse image series of human embryos fertilized in vitro were acquired as anonymized sequences of human embryos donated to research with ethical approval from Coventry Research Ethics Committee (04/Q2802/26) and the Human Fertilisation and Embryology Authority (R0155). Embryos were cultured in 25 μL culture media (Origio, Redhill, United Kingdom) under mineral oil for up to 6 days, incubated at 37 °C in an atmosphere of 5% CO2, 5% O2, and 90% N2. The images were captured using the Embryoscope® system (Unisense Fertilitech, Copenhagen, Denmark), with up to seven focal depth planes, 15–25 μm apart, recorded at 20-min intervals using a Hoffman modulation contrast (HMC) optical setup (25) and a 635 nm LED as light source. Fresh medium was supplied at intervals, but embryos were otherwise undisturbed during imaging. The total dataset consisted of image series of 39 embryos from seven different couples, of which 28 developed into blastocysts. Fourteen series of embryos (of which nine developed to blastocysts) were used in an initial study (referred to as training set) to optimize algorithm parameters, and the analysis was repeated using the same parameters for the remaining 25 embryos (of which 18 developed blastocysts). The latter is referred to as the test set.

Software Implementation

Series of stacks of HMC images with a gray scale ranging from 0 to 255 provided the raw material for this study. In HMC microscopy, changes in optical path length are optically converted to light and dark gradients on an even gray background, resulting in an image where edges are the most prominent structures. As the number of edges in the image increases, the two dimensional distribution of image intensity changes. Objects in embryo development expected to result in an increased number of edges are visible nuclei and pronuclei as well as an increased number of blastomeres. Conversely, compaction and loss of focus are expected to increase image smoothness, following a loss of edge structures. Image variance is a measure of the distribution of gray levels within a specified region of the image and will increase with an increased number of edge structures. It is the hypothesis of this study that variance as a measure of edge structures can be used as an indirect method to identify the timing of embryo developmental stages.

To detect fluctuations in variance with sufficient sensitivity to distinguish changes caused by, for example, the appearance

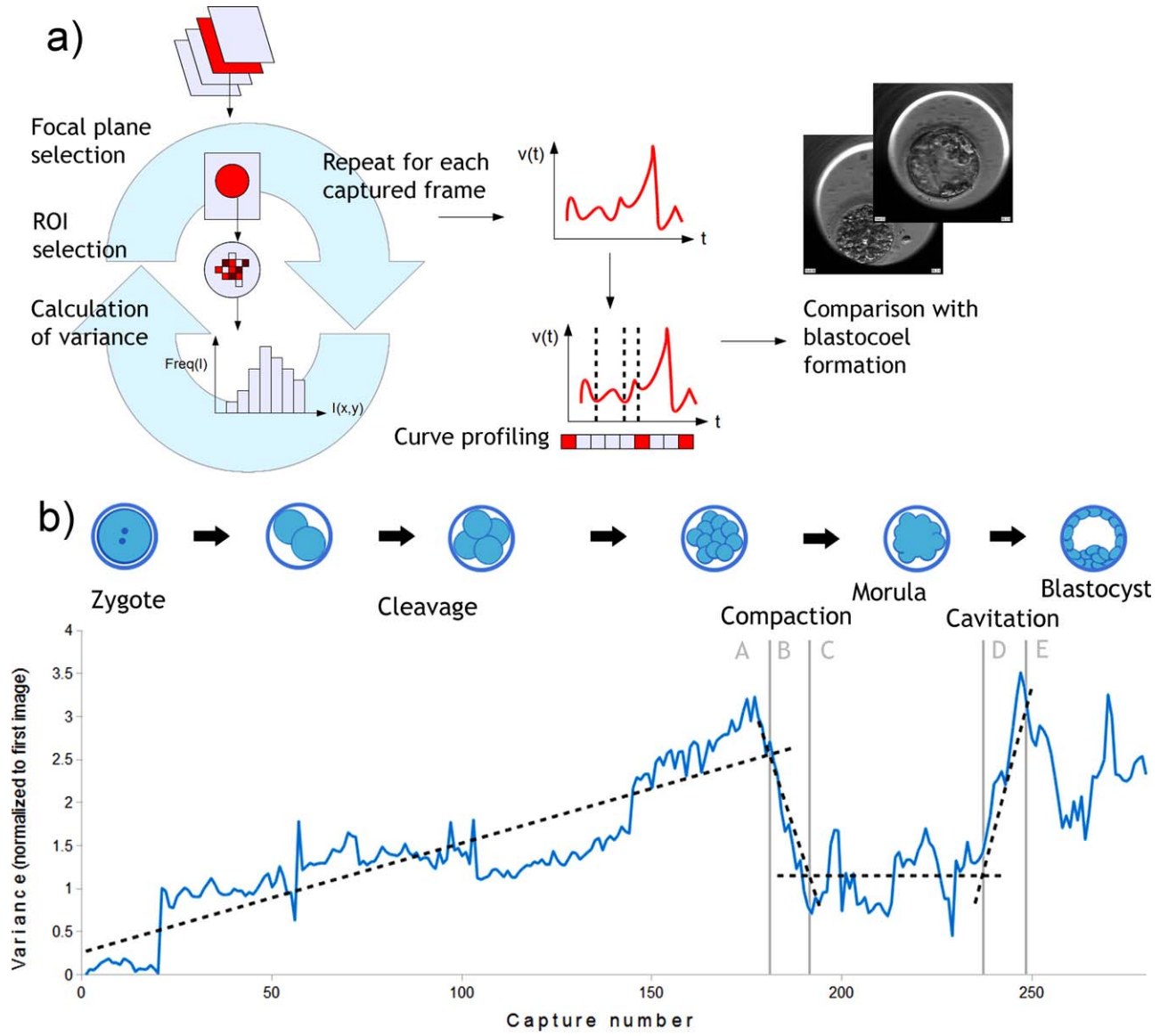

Figure 1. (**a**) Illustration of computational pipeline of the captured image series of an embryo. The optimal focal plane from the image stack was selected. A ROI was selected within each individual image, and one value of the variance in image intensity was computed for each ROI. This process was repeated for each capture in the image series, resulting in a function *v(t)* describing the variance as a function of time. *v(t)* was then further analyzed for the occurrence of detectable key events, profiling the embryo development. Finally, the profile for embryos forming blastocysts and not forming blastocysts were compared. (**b**) Image intensity variance of an embryo during the course of 280 frame captures, normalized to the first image in the series. Divisions during the cleavage stage are detectable as sudden increases in image variance, due to the number of increased edges in the image, as blastomeres undergo mitosis. At the onset of compaction, individual blastomere membranes are no longer distinguishable, and the variance drops and remains at a low level during the morula stage. The variance increases once more as blastocoel expansion sets in, and may fluctuate strongly during the blastocyst stage, if the embryo displays several cycles of collapse and re-expansion. The growth of the embryo has been considered in five stages: (A) Initial divisions from fertilization to onset of compaction. (B) Onset to completion of compaction. (C) Morula. (D) Cavitation. (E) Blastocyst. The mean and change in variance has been calculated for each section. Dashed trend lines have been added for illustrative purpose. [Color figure can be viewed in the online issue, which is available at wileyonlinelibrary.com.]

of a nucleus, two prefiltering steps were necessary. The first step, which was used for every image series, selected one focal level in the stack as containing the optimal focus. This resulted in a sequence of single captures (Fig. 1a). The process is described further in the Supporting Information (Appendix A). The second step, performed on each remaining capture, automatically detected the outline of the embryo using a circular Hough Transform. From the outline, the internal region of the embryo was selected as a circular ROI at half the embryo radius, as described in (26). The localized variance in image intensity was then calculated for the selected ROI of each image. Figure 2 shows an example of the breakdown of pronuclei and its effect on image variance. For the duration of the cleavage stage, it was assumed that no entire blastomere would

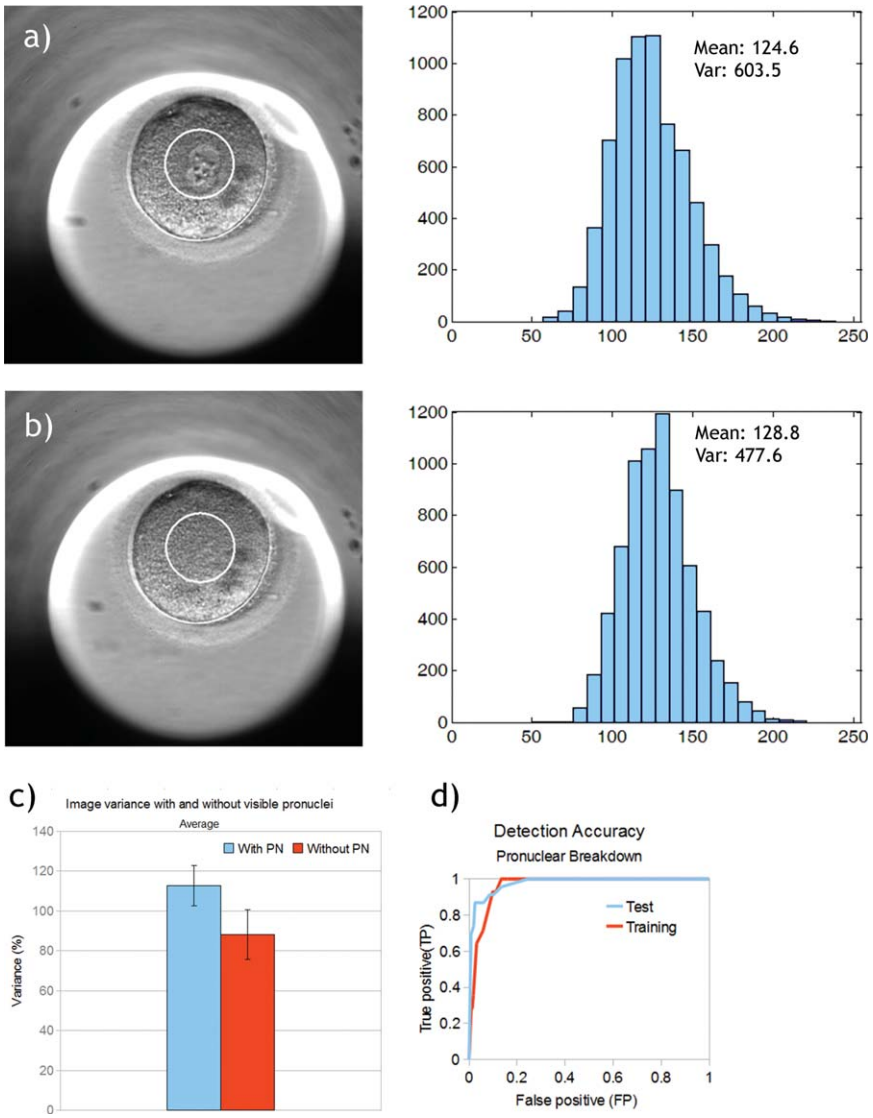

Figure 2. Calculation of variance in image intensity using pronuclei as an example. Images (**a**) and (**b**) were captured 20 min apart. The frequency of image gray scale values (0-255) within a selected ROI (white circle) at half embryo radius has been plotted as histograms, and the mean and variance calculated. (**c**) Difference in image variance before (blue) and after (red) PNB. Standard deviation calculated as mean over the training set of 14 embryos ($P < 0.0001$). (**d**) Detection accuracy of the training (14 embryos) and test (25 embryos) sets, respectively. The computation is governed by a single threshold (gradient of decreasing variance over time). PNB is defined as gradients larger than some threshold, yielding an increase in TP accuracy as the threshold decreases. [Color figure can be viewed in the online issue, which is available at wileyonlinelibrary.com.]

appear completely outside the ROI. For the blastocyst stage, the choice of region proved useful as the formation of the trophectoderm removed infocus blastomeres from the embryo interior to the outline of the blastocyst (outside the ROI), making the finished blastocyst appear with a characteristic drop in image variance, once the cavity was formed. Figure 1b shows an example of an embryo growing in vitro, as viewed with the image intensity variance of the embryo interior.

Next, images were examined visually for key occurrences in embryo development, and the same events were evaluated using the image variance, constructing two characteristic profiles of a growing embryo, one obtained by manual observation, and one by mathematical inspection. The accuracy of the hypothesis is defined by the correlation between the two profiles. The following details were included in the profile: the timing of the pronuclear breakdown (PNB) preceding syngamy, the timing of the first mitotic divisions up to eight-cell stage, and the transitions between a chosen set of main developmental stages. The details of the profiling are explained further in Supporting Information (Appendices B–D). A brief summary is given below.

Detection of Syngamy

For automatic detection of the PNB, a single threshold was optimized using the 14 training embryos. The timing of the PNB was computed for a number of thresholds, and the

minimum value giving 10% true positive (TP) detection (when comparing to visual inspection of the images of the training embryos) was selected and used for the testing embryos.

Cleavage Divisions

Mitotic divisions were also detected using a single threshold.

Compaction and Blastocyst Formation

Five stages were selected as being of interest: cleavage (A), compaction (B), morula (C), cavitation (D), and blastocyst (E) (Fig. 1b). The timing of transition between stages was defined as:

AB: main local maxima in variance, located before the main negative gradient.
BC: main negative gradient in variance.
CD: main positive gradient in variance, located after the main negative gradient.
DE: main local maxima in variance, located after the main negative gradient.

The computationally obtained stages and the transitions between stages were given letters to distinguish them from the visually defined embryo stages. For instance, the stage "B" is defined mathematically as the main negative gradient in variance, and it is part of the hypothesis that this relates to the formation of the compaction stage of the embryo. Finally, six traits for the developmental stages were combined and used simply to detect the presence or absence of a blastocoel. The six characteristics used were:

– The width (duration) of the negative gradient at compaction (B).
– The height of the maximum variance detected at the end of the cleavage stage (AB).
– The height of the maximum variance detected at cavitation (DE).
– The timing of compaction (B).
– The timing of the maximum at the end of the cleavage stage (AB).
– The total number of variance gradients during the entire development (a sign of strong fluctuating behavior, indicating poor quality).

The six traits were combined into four parameter sets, and the threshold for each one varied, while measuring the number of detected blastocyst formations.

Expert Validation and Statistical Analysis

Last, a total of 15 time-lapse image series from four different patients were used for validation. The timing of cell divisions and embryo stages was validated against the opinion of five expert clinical embryologists, each with at least 6 years of clinical embryology experience. The rest of the image series were annotated by the experimenters to the best ability using the same criteria as the embryologists. One image series was evaluated by all five experts, to allow direct comparison of their assessments. The annotation of timing in images was consistently within 1–3 time frames up to an eight-cell stage, and the overall quality of the embryo in 100% agreement (Fig. 3). *P* values equal or inferior to 0.05 was used for statistical significance. Intervals in graphs and for values are given as means ± SD unless otherwise stated.

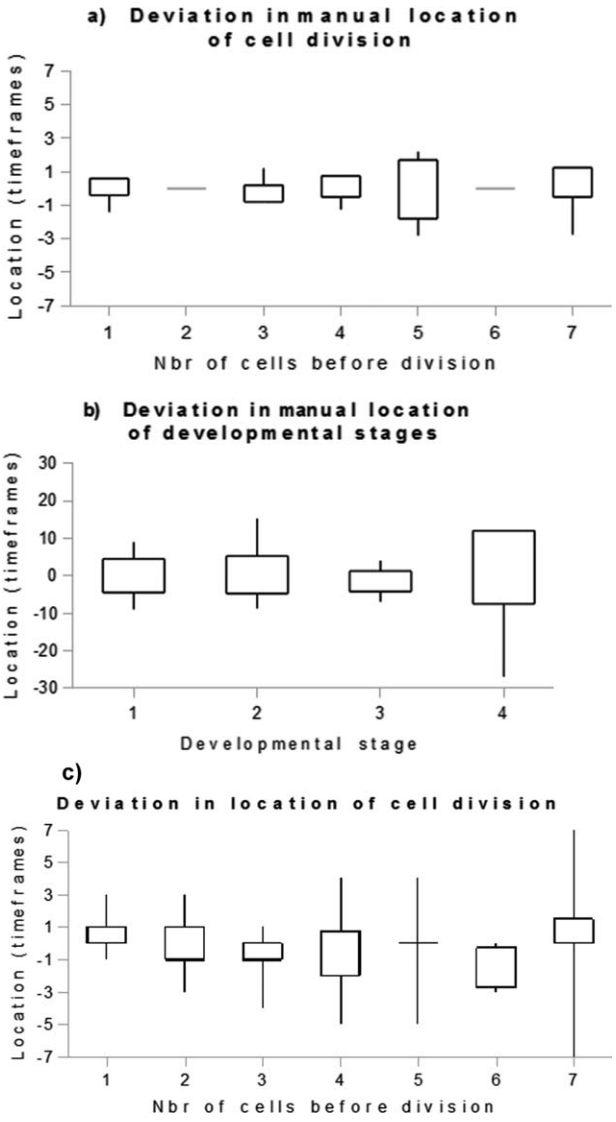

Figure 3. Standard deviation in manual annotation for the evaluation embryo in terms of (**a**) timings of mitotic divisions up to eight cells and (**b**) detection of the beginning of developmental stages: (1) Compaction, (2) Morula, (3) Cavitation, and (4) Blastocyst. Bars represent lower to upper quartile, whiskers minimum and maximum values. (**c**) The deviation from expert determined location of division in terms of timeframes for the divisions that were detected, plotted versus the number of cells preceding the division. Bars represent lower to upper quartile, whiskers minimum and maximum values.

Results

For embryos where developmental stages were visible in images, they were also reflected in the variance profile (Fig. 4). Both by manual observation and as measured by variance, large differences were apparent between individual embryos.

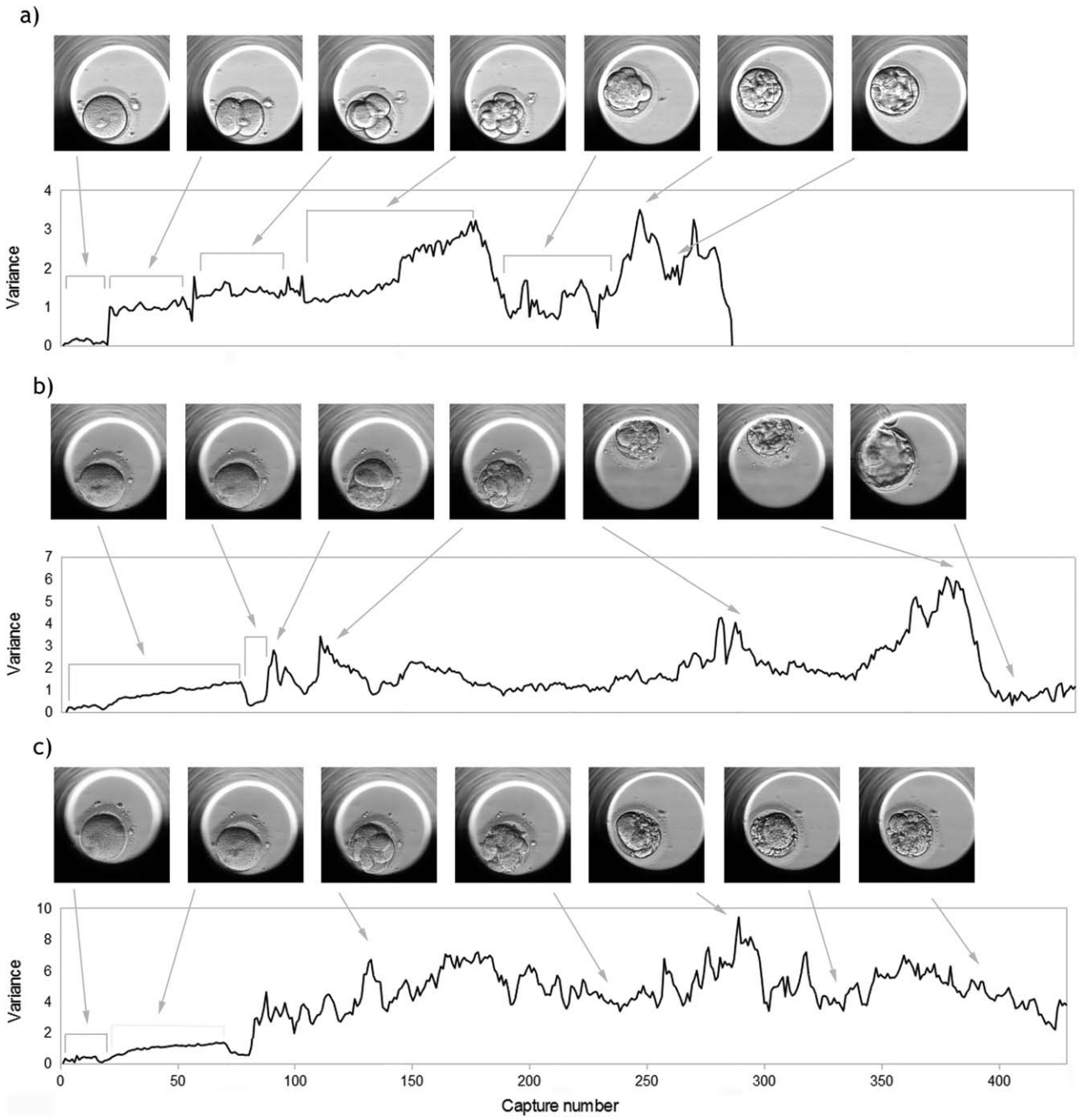

Figure 4. Profile of three representative embryos showing decreasing quality (**a–c**). Variance was calculated from the image intensity at a circular region encompassing the center of the embryo. A few example images are shown at points where characteristic changes are visible in the variance profile. For a good quality embryo (a), mitotic divisions are visible as successive increases in image variance, and the morula stage as a period of lowered variance. (b) illustrates a clearly expressed PNB, but experiences fragmentation during the cleavage stage, even though a blastocyst is eventually formed. In (c), the PNB is also apparent, but the embryo develops early fragments, never reaching a blastocyst stage.

Detection of Syngamy

In Figure 4b, the PNB is visible in the plot of variance versus image capture time as a sudden negative gradient over the course of 1–2 frames. Twenty images per embryo for the training set of 14 embryos were selected before and after PNB and used to profile the change of state. The difference in variance before and after the breakdown was large enough to be detectable, despite individual variation between images (Fig. 2c). The breakdown usually took less than one or two captures, giving an uncertainty of the timing of detection of at most 40 min at the current capture frequency. Requiring a 100% TP detection of the PNB for all 14 training embryos, the best overall result was 88% accuracy for the training embryos, and the inaccuracy being caused by false-positive

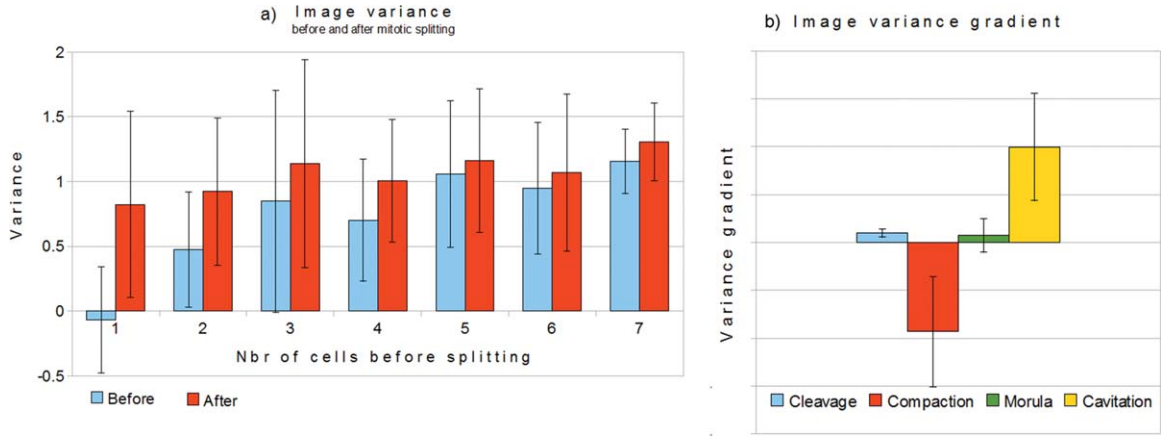

Figure 5. (**a**) Average variance for 14 training embryos before and after mitotic splitting. *P* values are $P < 0.05$ for first and second splitting, $P > 0.1$ for splitting 3–7. The negative variance before the first splitting is due to the drop in variance during syngamy. (**b**) Gradient of image variance for embryo developmental stages for the 14 training embryos. $P < 0.001$ for adjacent stages. [Color figure can be viewed in the online issue, which is available at wileyonlinelibrary.com.]

detection. Using the same settings for the 25 test embryos, an overall detection accuracy of 90% was achieved, with 91% TP detection (Fig. 2d).

Cleavage Divisions

In total, 37 of 39 image series had sufficient quality to detect the first five mitotic divisions. Two embryos were excluded because of heavy optical interference. For most time series, it was possible to use the first automatically detected cell divisions, but manual adjustments were made in a few cases where both the division between 2 and 3 cells and between 3 and 4 cells appeared within the 20-min gap between captures. Computational detection was compared to manual detection for divisions of up to the four- and eight-cell stages, as shown in Figure 5. For embryos at the 1–8-cell stage, there was a clear bias toward divisions being under detected when using the automated procedure. For embryos at 1–4 cells, no more than two false positives (detection of divisions that were not present) or false negatives (failure to detect divisions) occurred per time series. From Figure 3c, it is apparent that the uncertainty in the exact location of division increases with the number of blastomeres. From the total image set of 37 embryos, 100% of divisions from 1 to 2 cells were detected, 73% from 2 to 3 (or 4) cells, 30% from 3 to 4 cells, and 59% from 4 to 5 (or 6) cells. The three and five-cell stages were not always distinguishable using a image capture frequency of 20 min. Of all divisions between 1 and 6 cells, 62% of divisions were located at the same captured frame index using both computer and manual detection, and 76% of divisions were located within one captured frame index from the manually noted position. The same values for the manual detection, as compared to the mean of the expert annotation, were 35% exact location and 74% within one time frame. For the 28 embryos which eventually formed a blastocyst, a measurement was also made of the time elapsed between the automatically detected cell divisions from 2 to 3 cells and from 3 to 4 cells on the total set of 39 image series, resulting in 10.27 ± 2.66 h (2–3 cells), and 1.11 ± 1.34 h (3–4 cells), respectively.

Compaction and Blastocyst Formation

Manual annotation by experts showed less agreement on timing of transitions between developmental stages (Fig. 4b), compared to detection of division. For automatic detection, the mean and gradient of the variance for each of the Stages A–E was computed for each embryo. The results are shown in Figure 5. The change in variance per unit time during the compaction and the cavitation stage was one order of magnitude higher than that for the entire cleavage stage, typically 0.3 h^{-1}. All values showed a high degree of variation (commonly with standard deviations in the range of 60–80%) between embryos. Interestingly, there was a distinct difference between embryos from different patients, when the duration of the four stages A–D was measured (Fig. 6). The duration of the morula stage showed high variability among embryos from the same patient, whereas the duration of the cleavage stage and the cavitation stage had a higher interpatient than intrapatient variability. The compaction stage, morula stage, and cavitation stage had approximately the same duration, about 1/7 that of the cleavage stage. However, the duration of the cleavage stage was only approximately determined since the exact time of fertilization was unknown for the series analyzed. Finally, the detected transitions and relative height of variance local maxima and gradients were combined and used to classify each embryo in two groups, those forming blastocysts and those failing to do so. The results were evaluated by visual inspection of the captured image series. The best overall result was correct detection of a blastocyst being formed in 71.8% of cases but at a cost of 28.2% false-positive detection (computational indication of a blastocyst without actual blastocyst formation), with little sensitivity to parameter setting (Fig. 7).

Discussion

The method of locating the timing of mitotic divisions shows a larger span between maximum and minimum deviation from the true position compared to manual detection,

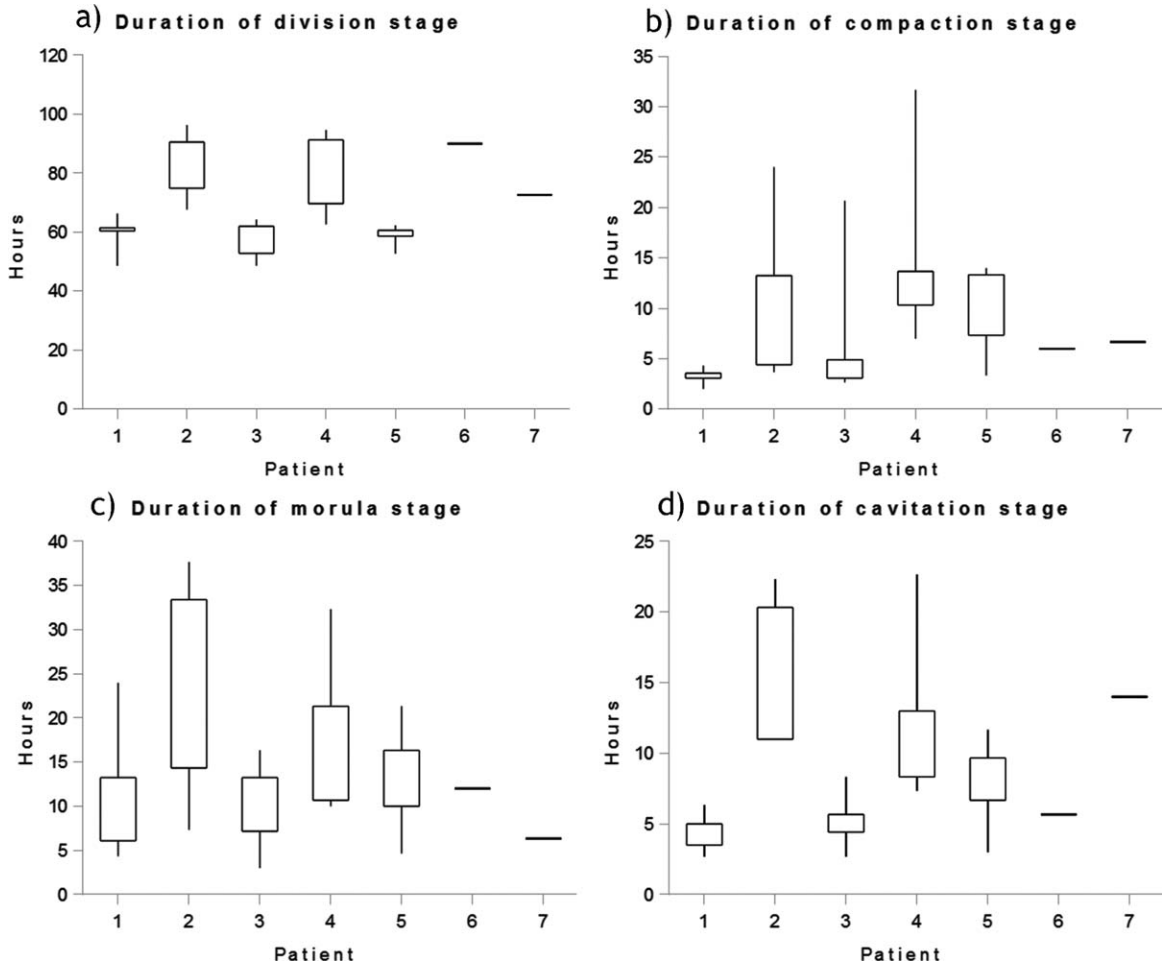

Figure 6. Duration in hours, automatically measured, of four stages of embryo development for seven patients (total 28 embryos). (**a**) Cleavage (the time from first frame to onset of compaction). (**b**) Compaction (time from onset until completed). (**c**) Duration of morula stage. (**d**) Duration of cavitation stage (time from onset of cavitation to blastocyst). Patients 6 and 7 had only one embryo each completing all four stages. Bars represent lower to upper quartile, whiskers minimum and maximum values.

but on average, our method performed better. 62% of cleavages identified by automatic detection were located at the exact same capture frame as manually identified by experts. The same agreement for manual detection between different experts was only 35%, showing the potential of automated image analysis to increase objectivity and consistency of embryo analysis. If instead, we define a correct detection to be within one captured frame of the control (corresponding to a timing inaccuracy of 20 min); the manual and computed accuracy were both approximately 75%. The results of the automatic method improved if only the 1–4-cell stages were considered, compared to all 1–8-cell stages. The results depend heavily on the frequency of image capture—20 min for this study—which was long enough for most cell divisions to take place over the course of several captured frames, but we experienced difficulty in distinguishing the three, five, and seven blastomere stages at this capture frequency. With more images captured and analyzed per unit time, it is possible that the uncertainty in location in terms of image index may increase, while at the same time decrease if computed for clock time. In measuring the timing of the first few mitotic divisions, the results overlap but have higher standard deviations than a previously reported study (27). However, the results for (27) were obtained with visual counting of mitotic divisions, whereas the timing of divisions in this study were automatically computed.

In detecting embryonic developmental stages, there were large variations between individual embryos, as expected from clinical experience. In spite of this, a clear trend in the variance profile was apparent, and we have shown that it was possible to identify the formation of a blastocyst by automated image analysis in >70% of cases. It was also apparent that the definition of stages and transitions using the localized variance was different from that of manual detection, indicating that this way of visualizing blastocyst development may serve best as a complement to inspection of images by eye.

The parameters for the detection of blastocyst formation depend on the frequency of image capture and the hardware settings, adding a requirement for a calibration stage before analysis. For future work, a comparison between different

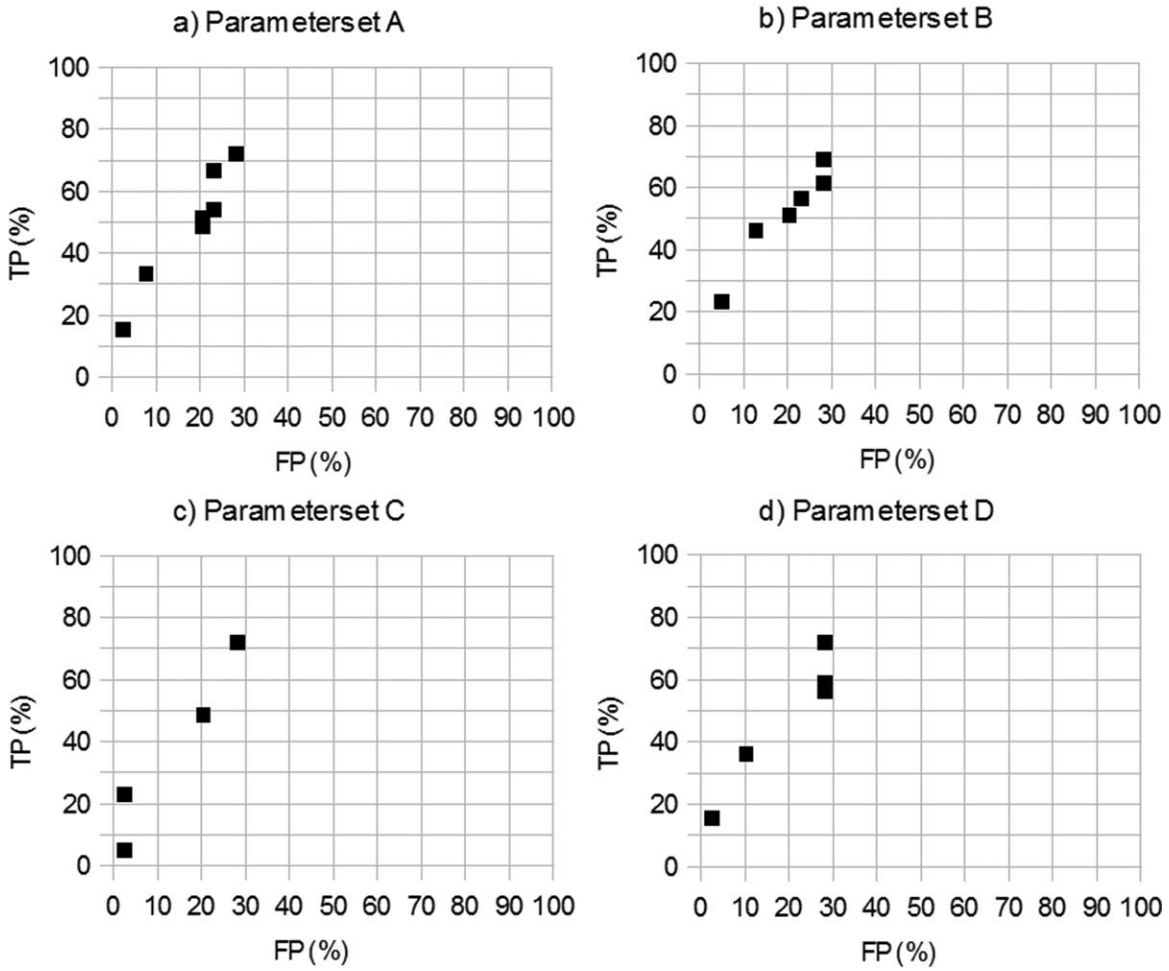

Figure 7. Example of the results in blastocoel detection using four different parameter sets. The parameters were: A: q1 = 20, q2 = 50, q3 = 0.65, q4 = 5, B: q1 = 20, q2 = 10, q3 = 0.65, q4 = 5, C: q1 = 20, q2 = 50, q3 = 0.65, q4 = 1, and D: q1 = 20, q2 = 50, q3 = 0.65, q4 = 10, where q1 is relative location of first main gradient, q2 is width of main gradient, q3 is height of the main maxima, and q4 is maximum number of gradients. Weights were w1 = 0.15, w2 = 0.15, w3 = 0.3, and w4 = 0.4 for all cases.

image capture frequencies would be desirable. It is also evident that the exact appearance of the variance function *v(t)* depended on the choice of the ROI. In this study, selecting a circular region of four different radii were investigated. Also, parameters for this study (Appendix D) were chosen as the most feasible using our current knowledge of embryo development. The implication of any choice of parameters should be further evaluated before taking on a larger scale study, as it is possible that new technical tools to study embryo will also require new methods to define embryo health. Furthermore, there is a trade- off between minimizing false-negative and false-positive detection. For our purpose of automating annotation, it was decided that false negatives were undesirable, whereas false positives could be acceptable and handled in a future manual or automatic filtering step. This decision may change depending on the intended purpose of detection. Also, to improve the accuracy, this framework could be expanded using more extractable image cues. For example, local image texture or measurements based on direct recognition of blastomere outlines could be used. Last, the use of an automatic image analysis is dependent on initial image quality, and for larger studies it will be necessary to establish robustness under clinical conditions.

There are reasons for caution in evaluating embryo quality as all studies of embryos before implantation will per definition only be able to assess embryo quality, not taking into account the uterine component of implantation. In IVF treatment, one or more embryos are normally selected for transfer to the uterus on Days 2–3 or 5–6 of development, when those developing in a normal and timely manner are usually at the four-cell, eight-cell or blastocyst stages, respectively. However, many embryos harbor abnormalities that render them incapable of prolonged development, and some of these abnormalities become manifest during preimplantation development as abnormal, delayed, or arrested growth. Thus, embryos transferred at the blastocyst stage are more likely to result in pregnancy than those transferred at earlier stages. Blastocyst transfer is, therefore, associated with a higher chance of

pregnancy and is the latest stage at which preimplantation selection can be carried out. Recent results (15) show that time-lapse studies of earlier embryonic stages can predict blastocyst development, but that the formation of a blastocyst is not necessarily an indication of a live birth outcome. In this study, we defined blastocyst formation to be evidence of a good quality embryo, but for future work we shall extend this study to clinical data where success in terms of initiating pregnancy and resulting in a live birth is known. Still, there is a need for prediction of blastocyst formation (28), and the ability for negative prediction, that is, deselection of unsuitable embryos, has the potential to save resources and allow for a more robust selection of single successful embryos for transfer. This could be achieved using automated analysis of previously identified parameters, such as immediate cleavage.

In conclusion, it is shown here that key events in preimplantation embryo development can be detected using a simple automated approach to embryo time-lapse image analysis, offering the potential of semiautomated annotation of clinical images on a large scale. The skills of the embryologist may then be better focused on checking and correcting a reduced number of uncertain computations, rather than performing routine manual annotation of the complete image set.

Acknowledgments

None of the data here would be of any use, if not checked and evaluated by Ben Lavender, Pavan Kachhwaha, and Dr. Deborah Taylor of the Centre for Reproductive Medicine, University Hospitals Coventry, and Warwickshire NHS Trust. In addition, Unisense Fertilitech helped greatly by providing images to complete the study. Finally, the authors would also like to thank Dr. Gabriela Czanner for invaluable help in evaluating the statistics.

Literature Cited

1. Schoolcraft WB, Gardner DK, Lane M, Schlenker T, Hamilton F, Meldrum DR. Blastocyst culture and transfer: Analysis of results and parameters affecting outcome in two in vitro fertilization programs. Fertil Steril 1999;72:604–609.
2. Sakkas D, Percival G, D'Arcy Y, Sharif K, Afnan M. Assessment of early cleaving in vitro fertilized human embryos at the 2-cell stage before transfer improves embryo selection. Fertil Steril 2001;76:1150–1156.
3. Guerif F, Le GA, Giraudeau B, Poindron J, Bidault R, Gasnier O, Royere D. Limited value of morphological assessment at days 1 and 2 to predict blastocyst development potential: A prospective study based on 4042 embryos. Hum Reprod 2007;22:1973–1981.
4. Racowsky C, Vernon M, Mayer J, Ball GD, Behr B, Pomeroy KO, Wininger D, Gibbons W, Conaghan J, Stern JE. Standardization of grading embryo morphology. J Assist Reprod Genet 2010;27:437–439.
5. Jurisica I, Mylopoulos J, Glasgow J, Shapiro H, Casper RF. Case-based reasoning in IVF: Prediction and knowledge mining. Artif Intell Med 1998;12:1–24.
6. Manna C, Patrizi G, Rahman A, Sallam H. Experimental results on the recognition of embryos in human assisted reproduction. Reprod Biomed Online 2004;8:460–469.
7. Patrizi G, Manna C, Moscatelli C, Nieddu L. Pattern recognition methods in human-assisted reproduction. Int Trans Oper Res 2004;11:365–379.
8. Kawamoto K, Houlihan CA, Balas EA, Lobach DF. Improving clinical practice using clinical decision support systems: A systematic review of trials to identify features critical to success. Br Med J 2005;330:765.
9. Morales DA, Bengoetxea E, Larrañaga P, García M, Franco Y, Fresnada M, Merino M. Bayesian classification for the selection of in-vitro human embryos using morphological and clinical data. Comput Methods Programs Biomed 2008;90:104–116.
10. Sundvall L, Ingerslev HJ, Knudsen UB, Kirkegaard K. Inter- and intra-observer variability of time-lapse annotations. Hum Reprod 2013;28:3215–3221.
11. Azzarello A, Hoest T, Mikkelsen AL. The impact of pronuclei morphology and dynamicity on live birth outcome after time-lapse culture. Hum Reprod 2012;27:2649–2657.
12. Basile N, Meseguer M. Time-lapse technology: Evaluation of embryo quality and new markers for embryo selection. Expert Rev Obstet Gynecol 2012;7:175–190.
13. Cruz M, Garrido N, Herrero J, Pérez-Cano I, Muñoz M, Meseguer M. Timing of cell division in human cleavage-stage embryos is linked with blastocyst formation and quality. Reprod Biomed Online 2012;25:371–381.
14. Kirkegaard K, Agerholm IE, Ingerslev HJ. Time-lapse monitoring as a tool for clinical embryo assessment. Hum Reprod 2012;27:1277–1285.
15. Kirkegaard K, Kesmodel US, Hindkjær JJ, Ingerslev HJ. Time-lapse parameters as predictors of blastocyst development and pregnancy outcome in embryos from good prognosis patients: A prospective cohort study. Hum Reprod 2013;28:2643–2651.
16. Wong CC, Loewke KE, Bossert NL, Behr B, De Jonge CJ, Baer TM, Pera RAR. Non-invasive imaging of human embryos before embryonic genome activation predicts development to the blastocyst stage. Nat Biotechnol 2010;28:1115–1121.
17. Olsen NH. Morphology and Optics of Human Embryos from Light Microscopy.Department of Innovation, IT University of Copenhagen, 2004.
18. Giusti A, Corani G, Gambardella LM, Magli MC, Gianaroli L. Blastomere segmentation and 3D morphology measurements of early embryos from Hoffman Modulation Contrast image stacks. Rotterdam: IEEE Int Symp Biomed Imaging 2010; 1261−1264.
19. Agerholm IE, Hnida C, Cruger DG, Berg C, Bruun-Petersen G, Kølvraa S, Ziebe S. Nuclei size in relation to nuclear status and aneuploidy rate for 13 chromosomes in donated four cells embryos. J Assist Reprod Genet 2008;25:95–102.
20. Morales DA, Bengoetxea E. Automatic segmentation of zona pellucida in human embryo images applying an active contour model. Dundee, UK: Proceedings of the 12th Annual Conference on Medical Image Understanding and Analysis 2008;209–213.
21. Filho ES, Noble JA, Poli M, Griffiths T, Emerson G, Wells D. A method for semi-automatic grading of human blastocyst microscope images. Hum Reprod 2012;27:2641–2648.
22. Pedersen UD, Olsen, OF, Olsen, NH. A multiphase variational level set approach for modelling human embryos. In: Proceedings of the 2nd IEEE Workshop on variational, Geometric and Level Set Methods, 2003.
23. Hnida C, Engenheiro E, Ziebe S. Computer-controlled, multilevel, morphometric analysis of blastomere size as biomarker of fragmentation and multinuclearity in human embryos. Hum Reprod 2004;19:288–293.
24. Beuchat A, Thévenaz P, Unser M, Ebner T, Senn A, Urner F, Germond M, Sorzano COS. Quantitative morphometrical characterization of human pronuclear zygotes. Hum Reprod 2008;23:1983–1992.
25. Hoffman R. The modulation contrast microscope: Principles and performance. J Microsc 1977;110:205–222.
26. Mölder A, Czanner S, Costen N, Hartshorne G. Automatic detection of embryo location using rotational variance of the Hough Transform. 22nd International Conference of Pattern Recognition ICPR 2014, Stockholm, Sweden.
27. Chavez SL, Loewke KE, Han J, Moussavi F, Colls P, Munne S, Behr B, Reijo Pera RA. Dynamic blastomere behaviour reflects human embryo ploidy by the four-cell stage. Nat Commun 2012;3:1251.
28. Diamond MP, Willman S, Chenette P, Cedars MI. The clinical need for a method of identification of embryos destined to become a blastocyst in assisted reproductive technology cycles. J Assist Reprod Genet 2012;29:391–396.